# Joint Beamforming Design for RIS-Assisted Cell-Free Network with Multi-Hop Transmissions

Decai Shen, Zijian Zhang, and Linglong Dai*

**Abstract:** The collaboration of multiple Reconfigurable Intelligent Surfaces (RISs) and Access Points (APs) enjoys advantages of capacity enhancement, power saving, etc., making the RIS-assisted cell-free network an important architecture for future communications. Similar to most existing works on RIS-assisted communications, the multi-hop link among RISs, i.e., the reflecting link including more than one RISs, is usually ignored in RIS-assisted cell-free networks. In these scenarios, however, since multiple RISs are closely deployed, we find that the multi-hop channels should not be simply ignored due to their potential for capacity improvement. Unfortunately, to the best of our knowledge, there is no work exploring the multi-hop transmission of RIS-assisted cell-free networks. To fill in this blank, we investigate the multi-hop transmission of RIS-assisted cell-free networks, including the multi-hop channel model and the corresponding beamforming design. Specifically, we propose a general multi-hop transmission model, which takes the direct links, single-reflecting links, and multi-hop links into account. Based on this model, we formulate a beamforming design problem in an RIS-assisted cell-free network, which allows us to maximize the multi-user sum-rate with considering the impact of multi-hop channels. To address the non-convexity of the formulated problem, a joint active and passive beamforming scheme is proposed to solve the problem. Particularly, by utilizing fractional programming, we decouple the coupled beamforming parameters in the problem, and then these parameters are alternately optimized until the convergence of the sum-rate. Simulation results verify that the consideration for multi-hop links is necessary, and the capacity performance of the proposed scheme is 20% higher than those of the existing schemes.

**Key words:** Reconfigurable Intelligent Surface (RIS); cell-free network; multi-hop transmissions; beamforming

## 1 Introduction

Relying on the benefits of changing the propagation environment of wireless signals with low power consumption, Reconfigurable Intelligent Surface (RIS) has become one of the most attractive potential technologies for the future 6G wireless communications[1]. Composed of a large number of metamaterial-based passive elements, RIS has been widely adopted for several requirements including but not limited to overcoming the blockages[1], enhancing the system capacity[2, 3], acquiring the higher spectrum efficiency[4, 5], and achieving the energy-saving or massive-connecting transmissions[6, 7].

Most of the researches consider deploying the RISs in the cellular network, where all users in one cell are served by one Access Point (AP) with the assistance of one[8] or multiple[9] RISs. With the increase in cell density, the cellular network will face serious

● Decai Shen, Zijian Zhang, and Linglong Dai are with the Department of Electronic Engineering, Tsinghua University, Beijing 100084, China, and also with the Beijing National Research Center for Information Science and Technology (BNRist), Beijing 100084, China. E-mail: sdc18@mails.tsinghua.edu.cn; zhangzj20@mails.tsinghua.edu.cn; daill@tsinghua.edu.cn.
∗ To whom correspondence should be addressed.
  Manuscript received: 2023-02-28; revised: 2023-03-17; accepted: 2023-03-18

inter-cell interference, which plays a main role in limiting the system capacity. To solve this issue, another network scheme called the cell-free network[10] has been explored, in which all APs are scheduled to serve the user simultaneously. In this case, the cell boundary no longer exists and the inter-cell interference will be alleviated. Hence, we can increase the deployment density of APs to improve the system capacity. Nevertheless, the limitation is that, the increase in the APs number will introduce the explosion of hardware cost and power consumption.

Fortunately, the new scheme called RIS-assisted cell-free network[11–16] can effectively solve this problem, because the hardware cost and power consumption for the passive RISs are significantly lower than the active APs. To reduce the cost and acquire the little performance loss, we can replace a part of the existing APs with an equal amount of RISs and then introduce some more RISs in addition.

## 1.1 Prior work

As an emerging network architecture, the RIS-assisted cell-free network was proposed in Ref. [11], and has received extensive research interests[12–16]. Several works focused on beamforming designs[12, 13]. The authors in Ref. [12] have explored a low-complexity algorithm via the two-timescale transmission protocol to design the downlink beamforming at APs and RISs, where a Penalty Dual Decomposition (PDD) based method and a Primal-Dual Subgradient (PDS) based method were proposed for the beamforming at RISs and APs, respectively. In Ref. [13], to improve the uplink spectral efficiency of the RIS-assisted cell-free network, the Maximum Ratio (MR) and the Local Minimum Mean Squared Error (L-MMSE) combining methods have been proposed. Meanwhile, the channel estimation for RIS-assisted cell-free networks was explored in Ref. [14], where a generalized superimposed channel estimation scheme with the Generalized Superimposed Training (GST) method was proposed to minimize the channel estimation error statistics. Besides, the other valuable problems, like resource allocation and wireless energy transfer, have also acquired the researchers' attentions[15, 16]. The resource allocation problem in an RIS-assisted cell-free Non-Orthogonal Multiple Access (NOMA) networks was investigated in Ref. [15]. To maximize the energy efficiency, a novel hybrid Deep Deterministic Policy Gradient (DDPG) based algorithm was proposed, where a multi-agent DDPG framework was adopted for robustness enhancement. A detailed review of wireless energy transfer in RIS-assisted cell-free networks, including its potential application scenarios and system architecture, were proposed in Ref. [16].

These works explore the system architectures and show the potential benefits of RIS-assisted cell-free networks with satisfactory performance gains. Unfortunately, in these works, only the direct links, and the single-reflecting links (i.e., the transmission links from APs to the user via the reflection by a single RIS) are considered, while the multi-hop links (i.e., the transmission links departing from APs and reflected by multiple RISs until arriving to the user) are usually ignored. This is mainly because most of the existing works for RIS-assisted cell-free networks are inspired by RIS-assisted cellular networks, where there is only one RIS or a few RISs located in different regions with long distances. In this scenario for RIS-assisted cellular networks, multi-hop links can be assumed as nonexistent or negligible due to the serious path loss. Actually, this assumption has also been adopted by the existing RIS-assisted cell-free works[11–16].

However, in the RIS-assisted cell-free networks employed with multiple RISs and APs, the distances among different RISs could be pretty close, based on which the channels among RISs can not be ignored, and the existence of multi-hop links are reasonable. For the APs whose direct links and single-reflecting links are unsatisfactory, we can skillfully design the beamforming to utilize the multi-hop links, based on which the user can be efficiently served by more APs with beneficial received signals.

To the best of our knowledge, the existing works for RIS-assisted cell-free networks have not considered the important multi-hop transmission links[†], while these links are expected to effectively improve the transmission performance.

## 1.2 Our contributions

To explore the potential performance gain of RIS-assisted cell-free networks, we consider the multi-hop transmission in these networks and formulate a general multi-hop transmission model for RIS-assisted cell-free networks. Besides, we propose a corresponding joint beamforming scheme with considering the multi-hop transmission. The specific contributions of this paper

---

† Although the multi-hop transmission has not been studied in RIS-assisted cell-free networks, there are some existing works considering the multi-hop links in the RIS-assisted cellular networks[17–20]. However, it is difficult to transform these multi-hop transmission models into RIS-assisted cell-free networks, which will be discussed in detail in Section 2.2.

can be summarized as follows[‡].

Firstly, we explore the multi-hop transmissions for RIS-assisted cell-free networks by considering the direct links, single-reflecting links, and multi-hop links simultaneously. The multi-hop transmission model for RIS-assisted cell-free networks is also formulated. In most of the existing works related to multi-hop transmission for RIS-assisted cellular networks, the number of multi-hop paths, and the number of hop times (i.e., the number of reflecting times for a certain path) are usually limited. In this paper, a more general multi-hop model is explored, based on which reflection can be formulated between any two RISs without the restriction for the reflecting sequence, which is more suitable for the RIS-assisted cell-free scenario with multiple APs and RISs. In this regard, most of the existing multi-hop researches for RIS-assisted transmission can be treated as a special case of the proposed model.

Secondly, based on the multi-hop transmission model above, a joint beamforming design scheme is proposed for the active beamforming optimization at all APs and the passive beamforming optimization at all RISs with the existence of multi-hop links. The joint beamforming optimization for the RIS-assisted cell-free networks is formulated as a high-dimensional non-convex sum-rate maximization problem. To solve this issue, we utilize Lagrangian dual reformulation to divide the optimization procedure for active and passive beamforming. For the optimization of passive beamforming, the intractable difficulty is that the beamforming matrices for all RISs are coupled due to the existence of multi-hop links. Hence, we propose the Block Coordinate Descent (BCD) based scheme to decouple the beamforming for multiple RISs and optimize it for different RISs one by one. Then, for the non-convex active beamforming problem, we reformulate it with the Multidimensional Complex Quadratic Transform (MCQT) scheme and solve it with the Alternating Direction Method of Multipliers (ADMM) method.

Finally, we evaluate the proposed joint beamforming design scheme in the RIS-assisted cell-free network with multi-hop transmissions. Simulation results verify that the consideration for multi-hop links in the RIS-assisted cell-free network is necessary, and the performance of the proposed joint beamforming scheme is 20% higher than those of the existing schemes. Besides, for the

passive beamforming, we propose the beamforming design not only for ideal RIS but also for practical RIS with the constant modulus constraint, based on which we find that for RIS-assisted cell-free networks in our multi-hop scenario, the deployment for practical RISs with constant modulus constraint is enough and it can achieve the sum-rate close to the employment for ideal RISs.

## 1.3 Organization

For the rest of this paper, the multi-hop transmissions model and signal model are given in Section 2. In Section 3, the proposed joint beamforming scheme is proposed. In Section 4, we discuss the simulation results. In Section 5, we provide the conclusion of this paper.

## 2 System Model

In this section, we briefly introduce the architecture of the RIS-assisted cell-free network with multi-hop transmission at first. Then, the transmission model is given in detail, where the direct link, the single-reflecting link, and the multi-hop link are considered in this model. Finally, we give the channel model and signal model in the downlink multi-user scenario.

### 2.1 Architecture of system

The architecture of the multi-user communication network can be illustrated in Fig. 1. Scheduling by the Central Processing Unit (CPU), multiple APs and multiple RISs are deployed to simultaneously serve multiple users. Note that different from the cellular network, the user in the cell-free network can receive and utilize the signal sent or reflected from every AP and



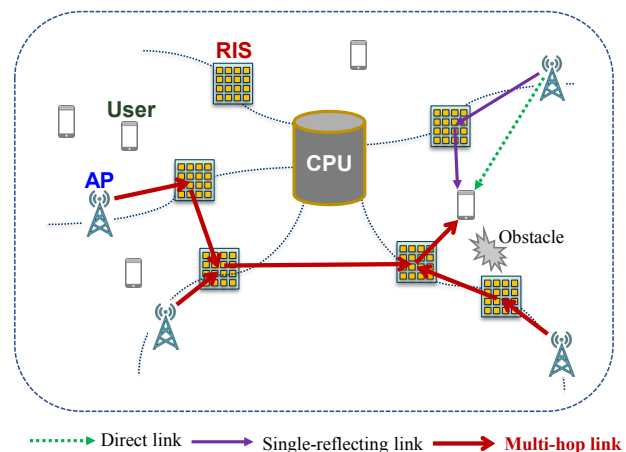**Fig. 1  System model for RIS-assisted cell-free network with multi-hop transmissions.**

---

‡ Simulation codes are provided to reproduce the results presented in this article: http://oa.ee.tsinghua.edu.cn/dailinglong/publications/publications.html.

every RIS. In this paper, we consider that there are $M$ APs (each AP employed by $A_T$ transmitting antennas), $R$ RISs (each RIS employed by $N$ passive elements), and $K$ users (each user employed by $A_R$ receiving antennas) in this communication network.

## 2.2 Multi-hop transmissions model

To the best of our knowledge, most all of the existing works for RIS-assisted cell-free networks only consider the direct and single-reflecting links. As discussed in Section 1, it is important to consider the multi-hop transmission model in RIS-assisted cell-free networks. It is worth pointing out that although the existence of multi-hop links has been confirmed and the corresponding multi-hop transmission models can be acquired in the valuable Refs. [17–20] for the RIS-assisted cellular networks, it is difficult to transform these transmission models into RIS-assisted cell-free networks. The main reason is that for most models of RIS-assisted cellular networks, usually only one AP needs to be considered, while there are multiple APs in the RIS-assisted cell-free networks.

To better explain this issue, we can summarize two limitations for the existing multi-hop transmission models in RIS-assisted cellular networks. Firstly, the number of multi-hop paths is usually limited. For one user, there is usually only one multi-hop path considered in the multi-hop transmission model like Refs. [17–19], and the number of the "hop" times is also preset. For example, there is only one $R$-hop path of the transmission model in the above works. Secondly, the sequence for the reflection is usually fixed rather than diverse. For example, the reflection started from the $i$-th RIS can only be pointed to the $j$-th RIS rather than others like $p$-th RIS[17–19]. Or as in Ref. [20], the transmission design can be achieved by building an oriented graph with multiple passive RISs and active RISs[21], based on which the reflection started from the $i$-th RIS can be pointed to $j$-th and $p$-th RIS, but the reflection from $j$-th or $p$-th RIS to the $i$-th RIS has to be ignored.

Those works are also meaningful because these two limitations have little effect on RIS-assisted cellular networks. For instance, there is only one AP in the system[20], so for the downlink transmission, it is straightforward to establish the reflection from the AP side to the user side instead of the opposite sequence.

However, for RIS-assisted cell-free networks, the above limitations of the existing multi-hop transmission will introduce serious effects, based on which existing models for RIS-assisted cellular networks are no longer applicable. Due to the existence of multiple APs, for one user, it is obvious that there will be several multi-hop paths from different APs. Besides, due to different distances between APs to the user, these multi-hop paths will have a different number of "hop" times (e.g., dual-hop, triple-hop, ..., and $R$-hop). Finally, the sequence for the reflection of different RISs should not be fixed due to the various positional relationships among APs, users, and RISs.

Hence, in this work, we formulate a more general multi-hop transmission model for the RIS-assisted cell-free networks, based on which the above limitations have been solved. This model is in line with the transmission for RIS-assisted cell-free networks, and most of the existing multi-hop researches for RIS-assisted cellular networks can be treated as a special case of the proposed model.

Specifically, the reflection exists in any two RISs, any RIS and AP, and any RIS and user. For one user, the transmission links can be divided into three parts: (1) the direct link, which is the transmission link directly from APs to the user; (2) the single-reflecting link, which is the transmission link from every AP to the user via single RIS's reflection; (3) the multi-hop link, which is the transmission link departing from every AP and reflected by multiple RISs until arriving to the user. Hence, the equivalent channel $\boldsymbol{H}_{m,k}^{\mathrm{H}} \in \mathbf{C}^{A_R \times A_T}$ between the $m$-th AP and the $k$-th user can be expressed as Eq. (1), shown at the bottom of this page, where $\overline{\boldsymbol{H}}_{m,k}^{\mathrm{H}} \in \mathbf{C}^{A_R \times A_T}$ represents the direct channel between the $m$-th AP and the $k$-th user, $\boldsymbol{P}_{t,k}^{\mathrm{H}} \in \mathbf{C}^{A_R \times N}$ represents the channel between the $t$-th RIS and $k$-th user, $\boldsymbol{G}_{m,t} \in \mathbf{C}^{N \times A_T}$

$$\boldsymbol{H}_{m,k}^{\mathrm{H}} = \underbrace{\overline{\boldsymbol{H}}_{m,k}^{\mathrm{H}}}_{\text{Direct link}} + \underbrace{\sum_{t=1}^{R} \boldsymbol{P}_{t,k}^{\mathrm{H}} \boldsymbol{\Theta}_t^{\mathrm{H}} \boldsymbol{G}_{m,t}}_{\text{Single-reflecting link}} +$$

$$\underbrace{\sum_{t' \neq t}^{R} \sum_{t=1}^{R} \boldsymbol{P}_{t',k}^{\mathrm{H}} \boldsymbol{\Theta}_{t'}^{\mathrm{H}} \boldsymbol{H}_{t',t} \boldsymbol{\Theta}_t^{\mathrm{H}} \boldsymbol{G}_{m,t} + \sum_{t'' \neq t,t'}^{R} \sum_{t' \neq t}^{R} \sum_{t=1}^{R} \boldsymbol{P}_{t'',k}^{\mathrm{H}} \boldsymbol{\Theta}_{t''}^{\mathrm{H}} \boldsymbol{H}_{t'',t'} \boldsymbol{\Theta}_{t'}^{\mathrm{H}} \boldsymbol{H}_{t',t} \boldsymbol{\Theta}_t^{\mathrm{H}} \boldsymbol{G}_{m,t} + \cdots}_{\text{Multi-hop links}} \qquad (1)$$

represents the channel between the $m$-th AP and $t$-th RIS, and $\boldsymbol{H}_{t',t} \in \mathbf{C}^{N \times N}$ is the channel between the $t$-th RIS and the $t'$-th RIS. $\boldsymbol{\Theta}_{t'} \in \mathbf{C}^{N \times N}$ is the passive beamforming matrix of the $t$-th RIS, which can be written as

$$\boldsymbol{\Theta}_t = \mathrm{diag}(\boldsymbol{\theta}_t) = \mathrm{diag}(\theta_{1,t}, \ldots, \theta_{n,t}, \ldots, \theta_{N,t}) \quad (2)$$

with $t \in \{1, 2, \ldots, R\}$, where $\boldsymbol{\theta}_t$ is the beamforming vector for the $t$-th RIS, and $\theta_{n,t} = \xi_{n,t}\mathrm{e}^{jp_{n,t}}$, $\xi_{n,t} \in [0,1]$ and $p_{n,t} \in [0, 2\pi]$ represents the amplitude and phase for the reflecting coefficient of the $n$-th element in the $t$-th RIS, respectively.

It can be found that a more general multi-hop transmission model is described according to Eq. (1). To better compare the difference between the proposed model and the existing model, a clear illustration can be shown according to Fig. 2. For most of the existing multi-hop scenarios, there is only one oriented multi-hop ($R$-hop) path between the AP and the user with the participation of all RISs. Under this limitation, one RIS will participate in the multi-hop process only one time. In the proposed model, there are several paths with the different number of "hop" times, including direct links, single-reflecting links, and various multi-hop links. Besides, the reflecting sequences between different RISs are diverse to ensure that there are more paths can be established between APs and users. For example, in Fig. 2, the reflection from RIS 1 to RIS 2 can be utilized to help AP 1 to serve User 1. At the same time, the reverse reflection of these two RISs can be utilized by AP 2 to serve User 2, based on which both of these two users can receive the signal from two APs simultaneously.

Meanwhile, for the various multi-hop transmissions scenario, the existing beamforming design scheme may be no longer effective. Hence, we propose the corresponding joint beamforming scheme in Section 3.

## 2.3 Channel model

In the following part, we introduce the model parameters of the above channels $\overline{\boldsymbol{H}}_{m,k}^{\mathrm{H}}$, $\boldsymbol{P}_{t,k}^{\mathrm{H}}$, $\boldsymbol{G}_{m,t}$, and $\boldsymbol{H}_{t',t}$. As widely adopted by the existing RIS-assisted wireless communication researches, Ref. [22] discussed the channel model with considering the path loss and small-scale fading to better describe the realistic relationship of the APs, RISs, and users. In this paper, we also adopt this channel model as follows. The small-scale fading channel between the RIS and the AP can be modeled as[22]

$$\boldsymbol{G} = \sqrt{\frac{\delta_{\mathrm{RA}}}{1 + \delta_{\mathrm{RA}}}} \boldsymbol{G}^{\mathrm{LoS}} + \sqrt{\frac{1}{1 + \delta_{\mathrm{RA}}}} \boldsymbol{G}^{\mathrm{NLoS}} \quad (3)$$

where $\delta_{\mathrm{RA}}$ is the Rician factor, $\boldsymbol{G}^{\mathrm{LoS}}$ represents the LoS channel, and $\boldsymbol{G}^{\mathrm{NLoS}}$ represents the NLoS Rayleigh fading channel. Similar models can be deployed for the channel between the user to the RIS, the channel between two RISs, and the channel between user and AP. The corresponding Rician factors are expressed as $\delta_{\mathrm{UR}}$, $\delta_{\mathrm{RR}}$, and $\delta_{\mathrm{UA}}$, respectively. Besides, we also describe the path loss between the RIS and the AP as[22]

$$L(d_{\mathrm{RA}}) = C_0 \left(\frac{d_{\mathrm{RA}}}{D_0}\right)^{-\rho_{\mathrm{RA}}} \quad (4)$$

where $d_{\mathrm{RA}}$ is the distance between the RIS and the AP, $C_0$ is the fiducial path loss with the distance as $D_0 = 1$ meter, and $\rho_{\mathrm{RA}}$ represents the path loss exponent between RIS and AP. Similar definitions can be extended to the path loss exponent between user and RIS $\rho_{\mathrm{UR}}$, between RIS and RIS $\rho_{\mathrm{RR}}$, and between user and AP $\rho_{\mathrm{UA}}$. The path loss for the other channels can also be calculated as $L(d_{\mathrm{UR}})$, $L(d_{\mathrm{RR}})$, and $L(d_{\mathrm{UA}})$. The specific values of the above parameters are also listed in Section 4 when we discuss the simulation results.

## 2.4 Signal model

We consider a downlink multi-user transmission
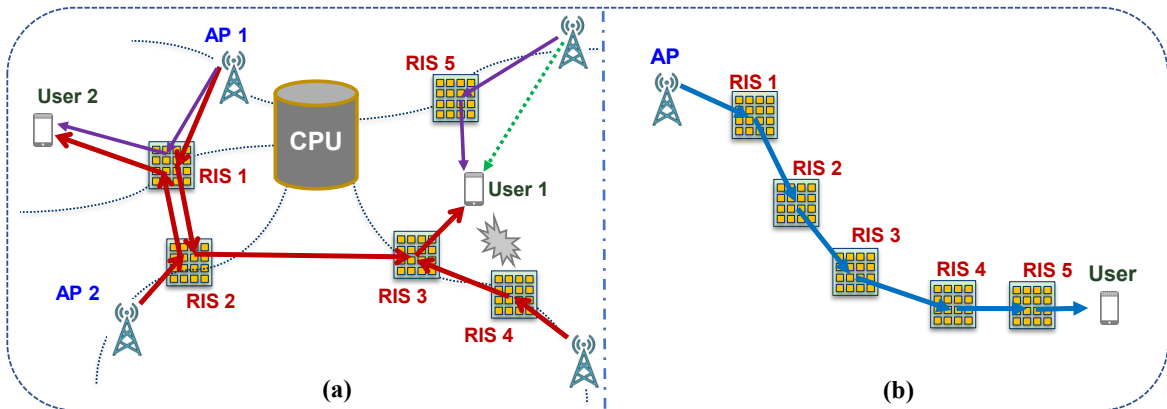


**Fig. 2    Clear comparison for the multi-hop transmission with the employment for five RISs. (a) Proposed RIS-assisted cell-free multi-hop transmission model and (b) existing multi-hop reflection model[17].**

scenario. In cell-free network scenario, all $M$ APs are synchronized to send the same transmitted signal, which means that one user will be served by all APs simultaneously. The transmitted signal in one AP with normalized power can be expressed as $s = [s_1, s_2, \ldots, s_K]^{\mathrm{T}}$. Before sending from the $m$-th AP, $s$ will be precoded with the AP active beamforming matrix $\boldsymbol{F}_m = [\boldsymbol{f}_{m,1}, \boldsymbol{f}_{m,2}, \ldots, \boldsymbol{f}_{m,K}] \in \mathbf{C}^{A_T \times K}$, based on which the precoded signal $\boldsymbol{x}_m \in \mathbf{C}^{A_T}$ of the $m$-th AP can be expressed as

$$\boldsymbol{x}_m = \sum_{j=1}^{K} \boldsymbol{f}_{m,j} s_j = \boldsymbol{F}_m s \quad (5)$$

Then, the precoded signal $\boldsymbol{x}_m$ will be sent from the $m$-th AP through the direct, single-reflecting, and the multi-hop links to the users. For the $k$-th user, the received signal $\boldsymbol{y}_{m,k} \in \mathbf{C}^{A_R}$ from the $m$-th AP is

$$\boldsymbol{y}_{m,k} = \boldsymbol{H}_{m,k}^{\mathrm{H}} \boldsymbol{x}_m + \boldsymbol{n}_{m,k} =$$
$$\boldsymbol{H}_{m,k}^{\mathrm{H}} \sum_{j=1}^{K} \boldsymbol{f}_{m,j} s_j + \boldsymbol{n}_{m,k} \quad (6)$$

where $\boldsymbol{n}_{m,k}$ is the equivalent received noise.

Note that at the same time, the precoded signal $\boldsymbol{y}_k \in \mathbf{C}^{A_R}$ from other $M-1$ APs will be received by the user, based on which the received signal of the $k$-th user from all APs can be expressed as

$$\boldsymbol{y}_k = \sum_{m=1}^{M} \boldsymbol{H}_{m,k}^{\mathrm{H}} \boldsymbol{x}_m + \boldsymbol{n}_k =$$
$$\sum_{m=1}^{M} \sum_{j=1}^{K} \boldsymbol{H}_{m,k}^{\mathrm{H}} \boldsymbol{f}_{m,j} s_j + \boldsymbol{n}_k =$$
$$\boldsymbol{u}_k s_k + \sum_{j=1, j \neq k}^{K} \boldsymbol{v}_{k,j} s_j + \boldsymbol{n}_k \quad (7)$$

where the vectors $\boldsymbol{u}_k$ and $\boldsymbol{v}_j$ can be expressed as

$$\boldsymbol{u}_k = \sum_{m=1}^{M} \boldsymbol{H}_{m,k}^{\mathrm{H}} \boldsymbol{f}_{m,k} \quad (8)$$

and

$$\boldsymbol{v}_{k,j} = \sum_{m=1}^{M} \boldsymbol{H}_{m,k}^{\mathrm{H}} \boldsymbol{f}_{m,j} \quad (9)$$

where $\boldsymbol{u}_k$ can be treated as $\boldsymbol{v}_{k,k}$, and $\boldsymbol{n}_k \sim \mathcal{CN}(\mu, \boldsymbol{\Upsilon}_k)$ is the additive white Gaussian noise at the receiver of user $k$ with $\mu = 0$ and $\boldsymbol{\Upsilon}_k = \sigma_k^2 \boldsymbol{I}_{A_R}$, where $\boldsymbol{I}_{A_R}$ is an identity matrix.

# 3 Problem Formulation and Proposed Joint Beamforming Design Scheme

In this section, we give the formulation for the

maximizing downlink sum-rate problem of the multi-hop RIS-assisted cell-free network at first. Then, the proposed joint beamforming design is discussed in detail, based on which the active beamforming at APs and the passive beamforming at RISs are iteratively optimized.

## 3.1 Problem formulation

According to the signal model in Section 2, for the multi-user scenario, we can express the downlink sum-rate as

$$R_{\mathrm{sum}} = \sum_{k=1}^{K} \log_2 \left| \boldsymbol{I}_{A_R} + \boldsymbol{U}_k (\boldsymbol{V}_k + \boldsymbol{\Upsilon}_k)^{-1} \right| \quad (10)$$

where $\boldsymbol{U}_k$ and $\boldsymbol{V}_k$ can be expressed as

$$\boldsymbol{U}_k = \sum_{m_1=1}^{M} \sum_{m_2=1}^{M} \boldsymbol{H}_{m_1,k}^{\mathrm{H}} \boldsymbol{f}_{m_1,k} \boldsymbol{f}_{m_2,k}^{\mathrm{H}} \boldsymbol{H}_{m_2,k} \quad (11)$$

and

$$\boldsymbol{V}_k = \sum_{j=1, j \neq k}^{K} \sum_{m_1=1}^{M} \sum_{m_2=1}^{M} \boldsymbol{H}_{m_1,k}^{\mathrm{H}} \boldsymbol{f}_{m_1,j} \boldsymbol{f}_{m_2,j}^{\mathrm{H}} \boldsymbol{H}_{m_2,k} \quad (12)$$

Hence, the originally optimization problem to maximize the downlink sum-rate under the constraint of transmission power at APs and the constraint of reflecting coefficients at RISs, can be formulated as follows:

$$\mathcal{P} : \max_{\hat{\boldsymbol{\Theta}}, \hat{\boldsymbol{F}}} R_{\mathrm{sum}} = \sum_{k=1}^{K} \log_2 \left| \boldsymbol{I}_{A_R} + \boldsymbol{U}_k (\boldsymbol{V}_k + \boldsymbol{\Upsilon}_k)^{-1} \right| \quad (13)$$

$$\text{s.t., } \mathrm{C}_1 : \theta_{n,t} \in \mathcal{T}_i, i \in \{1, 2\}, n \in \mathcal{I}(N), r \in \mathcal{I}(R) \quad (14)$$

$$\mathrm{C}_2 : \|\boldsymbol{F}_m\|_{\mathrm{F}}^2 \leqslant P_m, m \in \mathcal{I}(M) \quad (15)$$

Here, we have $\hat{\boldsymbol{\Theta}} = [\boldsymbol{\Theta}_1, \boldsymbol{\Theta}_2, \ldots, \boldsymbol{\Theta}_R]$ and $\hat{\boldsymbol{F}} = [\boldsymbol{F}_1, \boldsymbol{F}_2, \ldots, \boldsymbol{F}_M]$. $P_m$ denotes the maximum transmission power of the $m$-th AP. The integer sequence $\mathcal{I}(n)$ can be expressed as $\mathcal{I}(n) = \{0, 1, \ldots, n-1\}$, and $\mathcal{T}_i$ is the available set of the reflecting coefficients for RIS. There are two modes for $\mathcal{T}_i$ that match two mainstream hardware constructions of RIS in the existing researches as below.

**Mode 1 (Constant Modulus Constraint (CMC) mode):** The elements of $R$ RISs can only adjust the phase for the reflecting coefficient under the constant modulus constraint[23], based on which $\mathcal{T}_i$ can be expressed as

$$\mathcal{T}_1 = \{\theta_{n,t} \mid |\theta_{n,t}| = 1\}, t \in \mathcal{I}(R), n \in \mathcal{I}(N) \quad (16)$$

**Mode 2 (Ideal mode):** The elements of $R$ RISs are employed with more flexible hardware architecture,

which can adjust the reflecting coefficient not only for the phase but also for the amplitude[24], $\mathcal{T}_i$ can be expressed as

$$\mathcal{T}_2 = \{\theta_{n,t} \mid |\theta_{n,t}| \leqslant 1\}, t \in \mathcal{I}(R), n \in \mathcal{I}(N) \quad (17)$$

Both of the above two hardware designs are widely adopted in the existing RIS-assisted wireless communications, but the constraints of optimization problems introduced by RIS of these two modes are pretty different. Hence, in this paper, theses two modes are considered, seperately, based on which the corresponding optimization algorithms are proposed.

To solve Formulas (13)–(15), in the next subsection, the proposed joint beamforming design scheme to maximize the downlink sum-rate $R$ is discussed in detail.

## 3.2  Proposed joint beamforming design scheme

We can find that the original objective function Formula (13) is high-dimensional non-convex with the sum-logarithm operation for the fractional programming in matrix forms. Hence, we try to decouple the logarithm operation with an effective Lagrangian Dual Reformulation (LDR) method proposed in Ref. [25]. Besides, to avoid the complex matrix forms LDR due to the existence of the determinant, we perform a simple transformation for Eq. (10) at first. Specifically, by swapping the matrix sequence, we can rewritten Eq. (10) as

$$R_{\text{sum}} =$$
$$\sum_{k=1}^{K} \log_2 \left( 1 + \boldsymbol{u}_k^{\text{H}} \left( \sum_{j=1, j \neq k}^{K} \boldsymbol{v}_{k,j} \boldsymbol{v}_{k,j}^{\text{H}} + \boldsymbol{\Upsilon}_k \right)^{-1} \boldsymbol{u}_k \right) \quad (18)$$

Then, based on the LDR method, we can introduce an auxiliary vector $\boldsymbol{z}^{\text{T}} = [z_1, z_2, \ldots, z_K]$ and rewrite the original optimization problem $\mathcal{P}$ as

$$\mathcal{P}_1 : \max_{\hat{\boldsymbol{\Theta}}, \hat{\boldsymbol{F}}, \boldsymbol{z}} R_1 \quad (19)$$
$$\text{s.t.,  Formulas (14) and (15)} \quad (20)$$

where the new objective function $R_1$ can be expressed as follows:

$$R_1 = \sum_{k=1}^{K} (1 + z_k) \boldsymbol{u}_k^{\text{H}} \left( \sum_{j=1}^{K} \boldsymbol{v}_{k,j} \boldsymbol{v}_{k,j}^{\text{H}} + \boldsymbol{\Upsilon}_k \right)^{-1} \boldsymbol{u}_k -$$
$$\sum_{k=1}^{K} z_k + \sum_{k=1}^{K} \log_2(1 + z_k) \quad (21)$$

From Eq. (21) we can find that the optimizable parameters $\hat{\boldsymbol{\Theta}}$ and $\hat{\boldsymbol{F}}$ have been "moved" out from the logarithm, based on which we can optimize $\mathcal{P}_1$ with more alternative solutions compared with the original problem $\mathcal{P}$.

To solve the equivalent problem $\mathcal{P}_1$, we can iteratively optimize the variables $\hat{\boldsymbol{\Theta}}$, $\hat{\boldsymbol{F}}$, and $\boldsymbol{z}$. When we optimize one of the variables, the remaining variables are set as fixed values. In the following part, we give the optimized method of the above variables proposed in our beamforming design scheme.

### 3.2.1  Optimization for the passive beamforming $\hat{\boldsymbol{\Theta}}$

Firstly, we discuss the optimization procedure for passive beamforming $\hat{\boldsymbol{\Theta}}$. With the fixed $\hat{\boldsymbol{F}}^{\star}$ and $\boldsymbol{z}^{\star}$, we can reformulated $\mathcal{P}_1$ as

$$\mathcal{P}_2 : \max_{\hat{\boldsymbol{\Theta}}} R_2 \quad (22)$$
$$\text{s.t., Formula (14)} \quad (23)$$

where $R_2$ can be expressed as

$$R_2(\hat{\boldsymbol{\Theta}}) = \sum_{k=1}^{K} (1 + z_k^{\star}) \boldsymbol{u}_k^{\text{H}} \left( \sum_{j=1}^{K} \boldsymbol{v}_{k,j} \boldsymbol{v}_{k,j}^{\text{H}} + \boldsymbol{\Upsilon}_k \right)^{-1} \boldsymbol{u}_k \quad (24)$$

Although the logarithm operation has been removed by the above transformation, $\mathcal{P}_2$ is still intractable: Due to the existence of the matrix in Eq. (24), the fraction is high dimensional, which is difficult to be relaxed by the classical scale-form fractional programming method. To solve this issue, we adopt the MCQT[25], which extends the scale-form fractional programming to the matrix-form fractional programming. Specifically, by introducing a set of auxiliary variables $\boldsymbol{\alpha}_k \in \mathbf{C}^{A_R}, k \in \{1, 2, \ldots, K\}$ and $\boldsymbol{\alpha} = [\boldsymbol{\alpha}_1, \boldsymbol{\alpha}_2, \ldots, \boldsymbol{\alpha}_K]$, the problem $\mathcal{P}_2$ can be equivalently expressed as

$$\mathcal{P}_3 : \max_{\hat{\boldsymbol{\Theta}}, \boldsymbol{\alpha}} R_3 \quad (25)$$
$$\text{s.t., Formula (14)} \quad (26)$$

with $R_3$ given as

$$R_3(\hat{\boldsymbol{\Theta}}) = \sum_{k=1}^{K} \left( \sqrt{4(1 + z_k^{\star})} \text{Re}\{\boldsymbol{\alpha}_k^{\text{H}} \boldsymbol{u}_k\} - \boldsymbol{\alpha}_k^{\text{H}} \left( \sum_{j=1}^{K} \boldsymbol{v}_{k,j} \boldsymbol{v}_{k,j}^{\text{H}} + \boldsymbol{\Upsilon}_k \right) \boldsymbol{\alpha}_k \right) \quad (27)$$

Formula (25) can be solved by optimizing $\boldsymbol{\alpha}$ and $\hat{\boldsymbol{\Theta}}$, seperately. Firstly, with a fixed $\hat{\boldsymbol{\Theta}}^{\star}$, the optimal value of $\boldsymbol{\alpha}$ can be calculated by $\partial R_3 / \partial \boldsymbol{\alpha}_k = 0$ for $k \in \{1, 2, \ldots, K\}$. According to the derivatives operation, we can acquire

$$\boldsymbol{\alpha}_k^{\text{opt}} = \sqrt{1 + z_k^{\star}} \left( \sum_{j=1}^{K} \boldsymbol{v}_{k,j} \boldsymbol{v}_{k,j}^{\text{H}} + \boldsymbol{\Upsilon}_k \right)^{-1} \boldsymbol{u}_k \quad (28)$$

Then, to solve the optimization for $\hat{\boldsymbol{\Theta}}$ with a fixed $\boldsymbol{\alpha}^\star$, we can rewrite Formulas (25) and (26) as

$$\mathcal{P}_4 : \max_{\hat{\boldsymbol{\Theta}}} \quad R_4 \tag{29}$$

$$\text{s.t., Formula (14)} \tag{30}$$

with $R_4$ as

$$R_4(\hat{\boldsymbol{\Theta}}) = \sum_{k=1}^{K} \sqrt{4(1+z_k^\star)}\mathrm{Re}\{g(k,k)\} - \\ \sum_{k=1}^{K}\sum_{j=1}^{K} g(k,j)g^*(k,j) \tag{31}$$

where the new function $g(k,j)$ can be expressed as Eq. (32), shown at the bottom of this page, where (*a*) holds by the channel model according to Eq. (1). The difficulty in solving this problem $\mathcal{P}_4$ to optimize $\hat{\boldsymbol{\Theta}}$ is that, there are more than one RISs in the RIS-assisted cell-free system, and the beamforming matrices of different RISs are coupled as shown in Eq. (32). Hence, most of the existing schemes for the passive beamforming design can not solve this problem with satisfactory performance, where usually only one RIS or several uncoupled RISs are considered. In this paper, we divide the coupled beamforming matrices to alternately optimize the beamforming of $R$ RISs in turn. Specifically, when we want to discuss the optimization for the $r$-th RIS, $g(k,j)$ can be rewritten as Eq. (33), shown at the bottom of the page.

For the optimization of the $r$-th RIS beamforming, we will treat only $\boldsymbol{\Theta}_r$ as the optimizable variable while treating other beamforming matrices as fixed parameters. By substituting Eq. (33) into Eq. (31), we can formulate

the optimized problem for the $r$-th RIS as

$$\mathcal{P}_{\mathrm{RIS}} : \max_{\boldsymbol{\theta}_r} \quad R_{\mathrm{RIS}}(\boldsymbol{\theta}_r) \tag{34}$$

$$\text{s.t.,} \quad \theta_{n,r} \in \mathcal{T}_i, i \in \{1,2\}, n \in \mathcal{I}(N) \tag{35}$$

with $R_{\mathrm{RIS}}$ as

$$R_{\mathrm{RIS}}(\boldsymbol{\theta}_r) = -\boldsymbol{\theta}_r^{\mathrm{H}}\boldsymbol{\Psi}\boldsymbol{\theta}_r + \mathrm{Re}\{2\boldsymbol{\theta}_r^{\mathrm{H}}\boldsymbol{\varrho}\} \tag{36}$$

where

$$\boldsymbol{\Psi} = \sum_{k=1}^{K}\sum_{j=1}^{K} \boldsymbol{\psi}_{k,j}\boldsymbol{\psi}_{k,j}^{\mathrm{H}},$$

$$\boldsymbol{\varrho} = \sqrt{1+z_k^\star}\boldsymbol{\psi}_{k,j} - \sum_{k=1}^{K}\sum_{j=1}^{K} \boldsymbol{\psi}_{k,j}\tau_{k,j}^* \tag{37}$$

where $\boldsymbol{\psi}_{k,j}$ and $\tau_{k,j}$ can be acquired according to Eq. (33), and $\tau_{k,j}^*$ represents the conjugate value for $\tau_{k,j}$. From the expression for $R_{\mathrm{RIS}}$ in Eq. (36), it is worth noticing that $\mathcal{P}_{\mathrm{RIS}}$ is easy to be solved, since the $\boldsymbol{\Psi}$ is positive semidefinite and the objective function is convex. For the two mainstream modes for hardware construction of RIS[23, 24], we adopt the different optimization algorithms respectively.

**Case 1:** For the $\mathcal{T}_2$ mode, where RIS can adjust the reflecting coefficient not only for the phase but also for the amplitude, as shown in Eq. (16), $\mathcal{P}_{\mathrm{RIS}}$ is convex since the constraint in Formula (35) is convex with $i = 2$. Hence, many existing convex optimization schemes, like alternating direction method of multipliers[26], can de adopted with the help of CVX Toolbox.

**Case 2:** For the $\mathcal{T}_1$ mode, where RIS can only adjust the phase for the reflecting coefficient, as shown in Eq. (16), $\mathcal{P}_{\mathrm{RIS}}$ is non-convex under the constant modulus constraint of Formula (35) with $i = 1$. In this case, we

$$g(k,j) = \boldsymbol{\alpha}_k^{\star\mathrm{H}}\boldsymbol{v}_{k,j} = \boldsymbol{\alpha}_k^{\star\mathrm{H}}\sum_{m=1}^{M} \boldsymbol{H}_{m,k}^{\mathrm{H}}\boldsymbol{f}_{m,j}^\star \overset{(a)}{=}$$

$$\boldsymbol{\alpha}_k^{\star\mathrm{H}}\sum_{m=1}^{M}\left(\overline{\boldsymbol{H}}_{m,k}^{\mathrm{H}} + \sum_{t=1}^{R} \boldsymbol{P}_{t,k}^{\mathrm{H}}\boldsymbol{\Theta}_t^{\mathrm{H}}\boldsymbol{G}_{m,t} + \sum_{t'\neq t}^{R}\sum_{t=1}^{R} \boldsymbol{P}_{t',k}^{\mathrm{H}}\boldsymbol{\Theta}_{t'}^{\mathrm{H}}\boldsymbol{H}_{t',t}\boldsymbol{\Theta}_t^{\mathrm{H}}\boldsymbol{G}_{m,t} + \cdots\right)\boldsymbol{f}_{m,j}^\star \tag{32}$$

$$g(k,j) \overset{(b)}{=} \boldsymbol{\alpha}_k^{\star\mathrm{H}}\sum_{m=1}^{M}\left(\boldsymbol{P}_{r,k}^{\mathrm{H}}\boldsymbol{\Theta}_r^{\mathrm{H}}\boldsymbol{G}_{m,r} + \sum_{t'\neq r}^{R} \boldsymbol{P}_{t',k}^{\mathrm{H}}\boldsymbol{\Theta}_{t'}^{\mathrm{H}}\boldsymbol{H}_{t',r}\boldsymbol{\Theta}_r^{\mathrm{H}}\boldsymbol{G}_{m,r} + \cdots\right)\boldsymbol{f}_{m,j}^\star +$$

$$\boldsymbol{\alpha}_k^{\star\mathrm{H}}\sum_{m=1}^{M}\left(\overline{\boldsymbol{H}}_{m,k}^{\mathrm{H}} + \sum_{t\neq r}^{R} \boldsymbol{P}_{t,k}^{\mathrm{H}}\boldsymbol{\Theta}_t^{\mathrm{H}}\boldsymbol{G}_{m,t} + \sum_{t'\neq t}^{R}\sum_{t\neq r}^{R} \boldsymbol{P}_{t',k}^{\mathrm{H}}\boldsymbol{\Theta}_{t'}^{\mathrm{H}}\boldsymbol{H}_{t',t}\boldsymbol{\Theta}_t^{\mathrm{H}}\boldsymbol{G}_{m,t} + \cdots\right)\boldsymbol{f}_{m,j}^\star \overset{(c)}{=}$$

$$\boldsymbol{\theta}_r^{\mathrm{H}}\sum_{m=1}^{M}\left(\mathrm{diag}(\boldsymbol{\alpha}_k^{\star\mathrm{H}}\boldsymbol{P}_{r,k}^{\mathrm{H}} + \sum_{t'\neq r}^{R} \boldsymbol{\alpha}_k^{\star\mathrm{H}}\boldsymbol{P}_{t',k}^{\mathrm{H}}\boldsymbol{\Theta}_{t'}^{\mathrm{H}}\boldsymbol{H}_{t',r})\boldsymbol{G}_{m,r}\boldsymbol{f}_{m,j}^\star\right) + \tau_{k,j} \overset{\triangle}{=}$$

$$\boldsymbol{\theta}_r^{\mathrm{H}}\boldsymbol{\psi}_{k,j} + \tau_{k,j} \tag{33}$$

adopt the majorization-minimization algorithm[27] to solve this non-convex problem. Specifically, the problem $\mathcal{P}_{\text{RIS}}$ with the objective function $R_{\text{RIS}}(\boldsymbol{\theta}_r)$ can be calculated as a series of sub-problems with the objective function $q(\boldsymbol{\theta}_r)$. Each sub-problem corresponds to one iteration. In the $(i+1)$-th iteration, we can calculate the sub-problem in the following:

$$\mathcal{P}_{\text{MM}} : \max_{\boldsymbol{\theta}_r} \quad q(\boldsymbol{\theta}_r|\boldsymbol{\theta}_r^i) \tag{38}$$

$$\text{s.t., Formula (35)} \tag{39}$$

where the objective function $q(\boldsymbol{\theta}_r|\boldsymbol{\theta}_r^i)$ can be defined as

$$R_{\text{RIS}}(\boldsymbol{\theta}_r) \geqslant q(\boldsymbol{\theta}_r|\boldsymbol{\theta}_r^i) \triangleq \boldsymbol{\theta}_r^{\text{H}} \boldsymbol{M} \boldsymbol{\theta}_r +$$
$$2\text{Re}\{\boldsymbol{\theta}_r^{\text{H}}(\boldsymbol{\Psi}-\boldsymbol{M})\boldsymbol{\theta}_r^i\}+$$
$$\boldsymbol{\theta}_r^{i\text{H}}(\boldsymbol{M}-\boldsymbol{\Psi})\boldsymbol{\theta}_r^i - 2\text{Re}\{2\boldsymbol{\theta}_r^{\text{H}}\boldsymbol{\varrho}\} \tag{40}$$

where $\boldsymbol{M} \triangleq \lambda_{\max}\boldsymbol{I}_N$, $\lambda_{\max}$ denotes the maximum eigenvalue of $\boldsymbol{\Psi}$, and $\boldsymbol{I}_N$ is an identity matrix. $\boldsymbol{\theta}_r^i$ is the optimized result in the $i$-th iteration. The advantage of the Majorization Minimization (MM) algorithm is that, for each iteration, we can acquire the closed-form optimum solution as

$$\boldsymbol{\theta}_r^{\star,i+1} = \exp(\text{j}\angle(\boldsymbol{\varrho}-\boldsymbol{\Psi}\boldsymbol{\theta}_r^i+\lambda_{\max}\boldsymbol{\theta}_r^i)) \tag{41}$$

Finally, by optimizing the $\boldsymbol{\theta}_r, r = [1, 2, \ldots, R]$, we can equivalently solve the intractable problem $\mathcal{P}_4$ in Formulas (29) and (30), based on which the optimization for $\hat{\boldsymbol{\Theta}}^{\text{opt}}$ can be achieved.

### 3.2.2 Optimization for the active beamforming $\hat{\boldsymbol{F}}$

In this part, we will discuss the optimization procedure for $\hat{\boldsymbol{F}}$. With the fixed $\hat{\boldsymbol{\Theta}}^{\star}$ and $\boldsymbol{z}^{\star}$, we can reformulated $\mathcal{P}_1$ as

$$\mathcal{P}_5 : \max_{\hat{\boldsymbol{F}}} \quad R_2 \tag{42}$$

$$\text{s.t., Formula (15)} \tag{43}$$

with $R_2$ as

$$R_2(\hat{\boldsymbol{F}}) = \sum_{k=1}^{K}(1+z_k^{\star})\boldsymbol{u}_k^{\text{H}}(\sum_{j=1}^{K}\boldsymbol{v}_{k,j}\boldsymbol{v}_{k,j}^{\text{H}}+\boldsymbol{\Upsilon}_k)^{-1}\boldsymbol{u}_k. \tag{44}$$

Note that the forms for Eqs. (44) and (24) are consistent, but the independent variables are different. Similar to the expression for $\mathcal{P}_3$ in Formulas (25) and (26), where a set of auxiliary variables $\boldsymbol{\alpha} = [\boldsymbol{\alpha}_1, \boldsymbol{\alpha}_2, \ldots, \boldsymbol{\alpha}_K]$ are introduced for the problem reformulation according to the MCQT scheme. To solve the problem $\mathcal{P}_5$, we also introduce a set of auxiliary variables $\boldsymbol{\beta} = [\boldsymbol{\beta}_1, \boldsymbol{\beta}_2, \ldots, \boldsymbol{\beta}_K]$ with $\boldsymbol{\beta}_k \in \mathbf{C}^{A_R}$. Similarly, with a fixed $\hat{\boldsymbol{F}}^{\star}$, the optimum value for $\boldsymbol{\beta}_k$ can be calculated as

$$\boldsymbol{\beta}_k^{\text{opt}} = \sqrt{1+z_k^{\star}}(\sum_{j=1}^{K}\boldsymbol{v}_{k,j}\boldsymbol{v}_{k,j}^{\text{H}}+\boldsymbol{\Upsilon}_k)^{-1}\boldsymbol{u}_k \tag{45}$$

Then, with a fixed $\boldsymbol{\beta}^{\star}$, we can rewrite the problem $\mathcal{P}_5$ to optimize $\hat{\boldsymbol{F}}$ as

$$\mathcal{P}_6 : \max_{\hat{\boldsymbol{F}}} \quad R_6 \tag{46}$$

$$\text{s.t., Formula (15)} \tag{47}$$

and we have

$$R_6(\hat{\boldsymbol{F}}) = \sum_{k=1}^{K}\sqrt{4(1+z_k^{\star})}\text{Re}\{\boldsymbol{\beta}_k^{\star\text{H}}\boldsymbol{u}_k\}-$$
$$\sum_{k=1}^{K}\sum_{j=1}^{K}\boldsymbol{\beta}_k^{\star\text{H}}\boldsymbol{v}_{k,j}\boldsymbol{v}_{k,j}^{\text{H}}\boldsymbol{\beta}_k^{\star} \overset{(a)}{=}$$
$$\text{Re}\{2\boldsymbol{\gamma}^{\text{H}}\tilde{\boldsymbol{f}}\} - \tilde{\boldsymbol{f}}^{\text{H}}\boldsymbol{\Lambda}\tilde{\boldsymbol{f}} \tag{48}$$

where $\tilde{\boldsymbol{f}} = [\boldsymbol{f}_{1,1}^{\text{H}}, \ldots, \boldsymbol{f}_{1,K}^{\text{H}}, \boldsymbol{f}_{2,1}^{\text{H}}, \ldots, \boldsymbol{f}_{M,K}^{\text{H}}]^{\text{H}}$ and $\boldsymbol{\gamma}^{\text{H}} = [\boldsymbol{\beta}_1^{\star\text{H}}\boldsymbol{H}_{1,1}^{\text{H}}, \ldots, \boldsymbol{\beta}_k^{\star\text{H}}\boldsymbol{H}_{m,k}^{\text{H}}, \ldots, \boldsymbol{\beta}_K^{\star\text{H}}\boldsymbol{H}_{M,K}^{\text{H}}]$, $\boldsymbol{\Lambda} \in \mathbf{C}^{A_T MK \times A_T MK}$ can be expressed as $\boldsymbol{\Lambda} = \boldsymbol{\gamma}\boldsymbol{\gamma}^{\text{H}}$. The existence for $(a)$ can be ensured by substituting Eqs. (8) and (9) into Eq. (48) ahead $(a)$. It is worth pointing out that based on this reformulation, $\mathcal{P}_6$ is a quadratically constrained quadratic program problem. Hence, we can solve this problem vis many existing optimization schemes like alternating direction method of multipliers[26].

Based on the above optimization, we can acquire the optimized value for the beamforming matrix $\hat{\boldsymbol{F}}^{\text{opt}}$ of $M$ APs.

### 3.2.3 Optimization for the auxiliary vector $z$

The optimization for $\boldsymbol{z}$ is intuitive. When we fix the values of $\hat{\boldsymbol{F}}^{\star}$ and $\hat{\boldsymbol{\Theta}}^{\star}$, the constraint conditions of $\mathcal{P}_1$ in Formulas (19) and (20) will be removed, based on which we can acquire the optimum $z_k^{\star}$ by derivatives operation $\partial R_1/\partial z_k = 0$ for $k \in \{1, 2, \ldots, K\}$ in Eq. (21) as

$$z_k^{\star} = \boldsymbol{u}_k^{\text{T}}(\sum_{j=1,j\neq k}^{K}\boldsymbol{v}_{k,j}^{*}\boldsymbol{v}_{k,j}^{\text{T}}+\boldsymbol{\Upsilon}_k)^{-1}\boldsymbol{u}_k^{*} \tag{49}$$

where $\boldsymbol{u}_k^{*}$ and $\boldsymbol{v}_{k,j}^{*}$ are the conjugate vectors for $\boldsymbol{u}_k$ and $\boldsymbol{v}_{k,j}$. According to Eq. (49), we can acquire the optimized value for the auxiliary vector $\boldsymbol{z}^{\text{opt}}$.

### 3.3 Summary for the proposed scheme

As discussed in Subsection 3.2, the optimization procedure for the proposed beamforming design scheme can be briefly summarized as follows. Firstly, the intractable original problem for the maximized sum-rate with sum-logarithm operation will be reformulated by introducing the auxiliary vector $\boldsymbol{z}$ with the help of the

LDR method. Then, the APs' beamforming $\hat{F}$ and the RISs' beamforming $\hat{\Theta}$ will be designed. Finally, the proposed scheme will be carried out by optimizing $z$, $\hat{F}$, and $\hat{\Theta}$ iteratively, as illustrated in Fig. 3.

# 4 Simulation Result

In this section, we discuss the simulation results for the proposed joint beamforming design scheme for the RIS-assisted cell-free network with multi-hop transmissions.

## 4.1 Simulation setup

**(1) Simulation scenario:** In this paper, we consider a classical cell-free network scenario[28] with the employment for multiple passive RISs, which is illustrated in Fig. 4. Specifically, an RIS-assisted cell-free network with 3 APs and 6 RISs are built in the Cartesian coordinate, and Fig. 4 is the vertical view. Three APs are placed in fixed positions. Six RISs are divided into two groups and randomly placed in two regions, which can be treated as the potential user regions in the realistic transmission environment, where the central coordinates of these two regions are (60, 5) and (100, 5). One or more users are randomly employed in
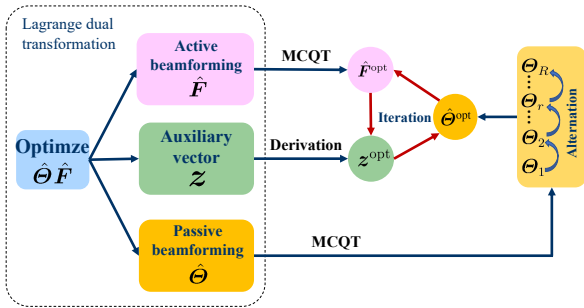


**Fig. 3 Optimization procedure for the proposed joint beamforming design scheme.**
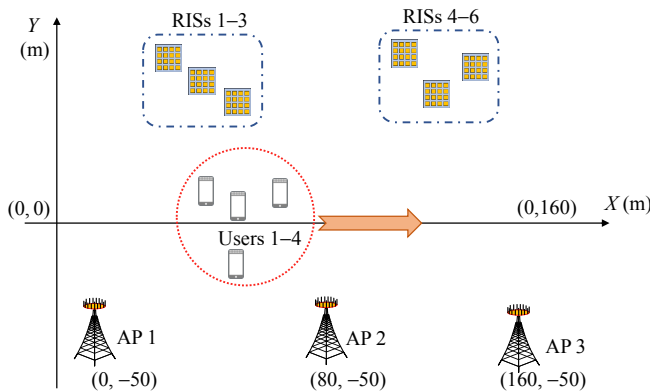


**Fig. 4 Illustration of the simulation scenario for the RIS-assisted cell-free network with 3APs, 6RISs, and 4 users.**

a circular region with diameter of 2 m, and the distance between center of the circle and the original point (0, 0) is with $0 < L < 160$ m.

**(2) Simulation parameters:** We list the simulation parameters adopted in this paper in the following Table 1.

**(3) Simulation baselines:** To evaluate the algorithm performance of the proposed joint beamforming scheme, we compare the proposed two schemes (considering the employment for RIS with the CMC mode and ideal mode) with the following baselines: (1) the RIS-assisted cell-free precoding framework proposed in Ref. [11], (2) the random RIS reflection, i.e., the passive beamforming for RISs are determined randomly and the active beamforming for APs are determined as the proposed scheme, and (3) the scenario without the RIS employment, i.e., the active beamforming for APs are determined as the proposed scheme.

## 4.2 Simulation results in the single-user case

In this subsection, we discuss the simulation results for the single-user case in the RIS-assisted cell-free network at first, i.e., all APs and RISs are scheduled to serve only one user.

Figure 5 illustrates the user rate against the maximum transmit power. This user is located at the circular region centered as (60, 0). From this figure we can find that the proposed scheme is superior to other baselines. Although the precoding framework in Ref. [11] is designed for RIS-assisted cell-free networks, they just consider the direct links and single-reflecting links, based on which the performance is unsatisfactory. Particularly, with $P_m = 20$ dBm, the proposed scheme is more 20% higher than the algorithm in Ref. [11]. This is mainly because that in the low-power case,

**Table 1 Simulation parameters.**

| Parameter | Value |
| --- | --- |
| Number of RISs | $R = 6$ |
| Number of APs | $M = 3$ |
| Number of users | $1 \leqslant K \leqslant 4$ |
| Number of elements at RIS | $N = 10$ |
| Number of antennas at AP | $A_T = 2$ |
| Number of antennas at user | $A_R = 2$ |
| Path loss exponent[22] | $\rho_{\mathrm{UR}} = 2.8, \rho_{\mathrm{RA}} = 2.5$ |
| Path loss exponent[22] | $\rho_{\mathrm{RR}} = 2.0, \rho_{\mathrm{UA}} = 3.5$ |
| Rician factor | $\delta_{\mathrm{UR}} = 0, \delta_{\mathrm{RA}} = \infty$ |
| Rician factor | $\delta_{\mathrm{RR}} = \infty, \delta_{\mathrm{UA}} = 0$ |
| Maximum transmission power | $20\,\mathrm{dBm} \leqslant P_m = P_{\max} \leqslant 40\,\mathrm{dBm}$ |
| Noise power | $\sigma_k^2 = -80$ dBm |
| Normalized path loss exponent | $C_0 = -30$ dB |

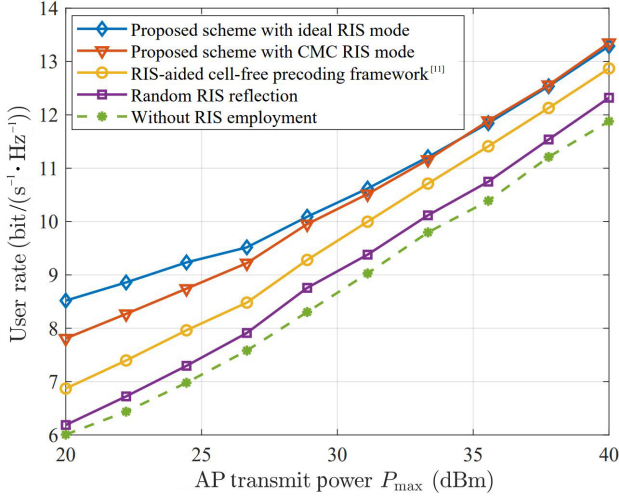**Fig. 5** **User rate against the AP transmission power in the single-user case.**

it is important to take full advantage of multi-hop transmissions by designing the passive beamforming of RISs.

In addition, we also consider the performance when the user locates in different positions as shown in Fig. 6, which corresponds to the different reflecting topology between the user, and the APs or RISs. The distance $L$ means the center of the circle for the user region from 0 to 160 m. We can find that in different locations, the user rate for the proposed schemes is higher than the other baselines. Besides, there are two peaks in $L = 60$ m and $L = 100$ m, where they are near the deployment regions for RISs. Without effective transmissions with the help of RISs, the performance for purple and green curves can only acquire a lower rate. With considering the single-reflecting transmission, the

performance for the algorithm in Ref. [11] is higher than the above curves. However, it still leaves a clear gap with our scheme, where the direct transmission, single-reflecting transmission and multi-hop transmission are integrally considered, based on which we can also find that the consideration for multi-hop links is necessary, since the multi-hop links are essential and equally important as the first two kinds of links.

### 4.3 Simulation results in the multi-user case

In this subsection, we discuss the simulation results for the multi-user case, where there has user interference should be considered. We set the number of users $K = 4$.

Figure 7 illustrates the sum-rate against the maximum transmit power in the multi-user case. There is an interesting point here that deserves to be discussed, i.e., with the increase of the AP transmission power, the performance gap between the proposed scheme and the algorithm in Ref. [11] widens significantly. The latter algorithm is even worse than the random RIS reflection. This is mainly because that the algorithm in Ref. [11] does not consider the multi-hop links which prominently exist in the transmission environment. Hence, in the multi-user case, the unbefitting beamforming design by Ref. [11] will result in the sharply increase in user interference especially in the high transmission power scenario.

Finally, we also discuss the sum-rate against the distance $L$ in the multi-user case as shown in Fig. 8. Firstly, in the deployment regions for RISs ($L = 60$ m and $L = 100$ m), the performance for the proposed scheme is significantly higher than the other baselines.
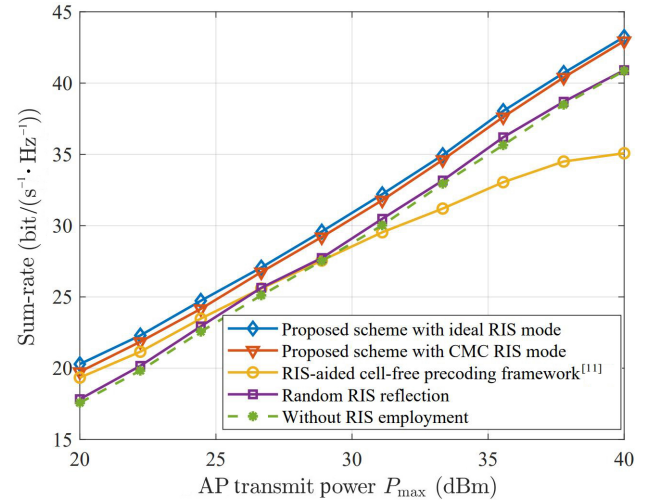


**Fig. 6** **User rate against the distance $L$ in the single-user case.**



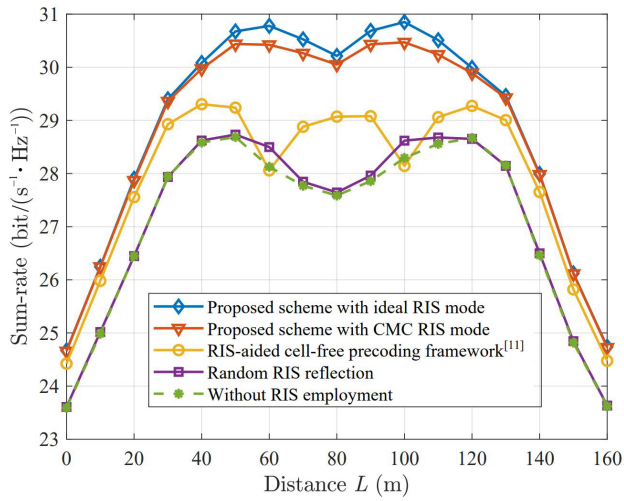**Fig. 7** **Sum-rate against the AP transmission power in the multi-user case.**

**Fig. 8** **Sum-rate against the distance *L* in the multi-user case.**

Especially, in these regions, the multi-hop links are stronger than the other regions due to the deployment for RISs, while the performance of the algorithm in Ref. [11] is decreasing since they do not consider the obvious multi-hop transmission. By the way, we can find that from Figs. 5–8, the performance for the proposed scheme with ideal RIS mode is slightly higher than the proposed scheme with CMC RIS mode. But this performance gap is acceptable in most scenarios, while the hardware cost for ideal RIS is significantly higher than the CMC RIS. This also provides the guides for RIS hardware selection according to the trade-off between the performance and hardware cost.

## 5 Conclusion

In this paper, we have investigated the RIS-assisted cell-free networks to improve the sum-rate performance. Different from most of the existing works that only consider the direct links and single-reflecting links, we have found that the multi-hop links are equally important as these two kinds of links. However, due to the existence of multiple APs and RISs, most of the existing multi-hop modes in RIS-assisted cellular networks are no longer appropriate in RIS-assisted cell-free networks. Hence, we have formulated a more general multi-hop transmission mode and proposed a joint beamforming scheme to maximize the sum-rate. We also leave the beam-tracking based multi-hop transmission in RIS-assisted cell-free network for future work, in which users can take advantage of the potential of multi-hop transmission with lower overhead in high-speed mobile scenarios.

## References

[1] C. Feng, W. Shen, J. An, and L. Hanzo, Joint hybrid and passive RIS-assisted beamforming for mmWave MIMO systems relying on dynamically configured subarrays, *IEEE Internet Things J.*, vol. 9, no. 15, pp. 13913–13926, 2022.

[2] H. Sun, S. Zhang, J. Ma, and O. A. Dobre, Time-delay unit based beam squint mitigation for RIS-aided communications, *IEEE Commun. Lett.*, vol. 26, no. 9, pp. 2220–2224, 2022.

[3] M. Wu, Z. Gao, Y. Huang, Z. Xiao, D. W. K. Ng, and Z. Zhang, Deep learning-based rate-splitting multiple access for reconfigurable intelligent surface-aided tera-hertz massive MIMO, *IEEE J. Sel. Areas Commun.*, vol. 41, no. 5, pp. 1431–1451, 2023.

[4] M. Jian and Y. Zhao, A modified off-grid SBL channel estimation and transmission strategy for RIS-assisted wireless communication systems, in *Proc. 2020 Int. Wireless Communications and Mobile Computing (IWCMC'20)*, Limassol, Cyprus, 2020, pp. 1848–1853.

[5] H. Liu, Y. Zhang, S. Gong, W. Shen, C. Xing, and J. An, Optimal transmission strategy and time allocation for RIS-enhanced partially WPSNs, *IEEE Trans. Wireless Commun.*, vol. 21, no. 9, pp. 7207–7221, 2022.

[6] J. Zhang, Z. Zheng, Z. Fei, and Z. Han, Energy-efficient multiuser localization in the RIS-assisted IoT networks, *IEEE Internet Things J.*, vol. 9, no. 20, pp. 20651–20665, 2022.

[7] X. Pang, N. Zhao, J. Tang, C. Wu, D. Niyato, and K. K. Wong, IRS-Assisted secure UAV transmission via joint trajectory and beamforming design, *IEEE Trans. Commun.*, vol. 70, no. 2, pp. 1140–1152, 2022.

[8] S. Liu, Z. Gao, J. Zhang, M. D. Renzo, and M. S. Alouini, Deep denoising neural network assisted compressive channel estimation for mmWave intelligent reflecting surfaces, *IEEE Trans. Veh. Technol.*, vol. 69, no. 8, pp. 9223–9228, 2020.

[9] M. Jian, R. Liu, E. Basar, Y. Liu, and C. Huang, Reconfigurable intelligent surface aided non-coaxial OAM transmission for capacity improvement, in *Proc. 2022 IEEE/CIC Int. Conf. Communications in China (ICCC'22)*, Foshan, China, 2022, pp. 594–599.

[10] E. Nayebi, A. Ashikhmin, T. L. Marzetta, and H. Yang, Cell-free massive MIMO systems, in *Proc. 49th Asilomar Conf. Signals, Systems and Computers*, Pacific Grove, CA, USA, 2015, pp. 695–699.

[11] Z. Zhang and L. Dai, A joint precoding framework for wideband reconfigurable intelligent surface-aided cell-free network, *IEEE Trans. Signal Process.*, vol. 69, pp. 4085–

4101, 2021.

[12] X. Gan, C. Zhong, C. Huang, Z. Yang, and Z. Zhang, Multiple RISs assisted cell-free networks with two-timescale CSI: Performance analysis and system design, *IEEE Trans. Commun.*, vol. 70, no. 11, pp. 7696–7710, 2022.

[13] E. Shi, J. Zhang, Z. Wang, D. W. K. Ng, and B. Ai, Uplink performance of RIS-aided cell-free massive MIMO system over spatially correlated channels, in *Proc. GLOBECOM 2022 – 2022 IEEE Global Communications Conf.*, Rio de Janeiro, Brazil, 2022, pp. 3259–3264.

[14] H. Ge, N. Garg, and T. Ratnarajah, Generalized superimposed channel estimation for uplink RIS-aided cell-free massive MIMO systems, in *Proc. 2022 IEEE Wireless Communications and Networking Conf.* (*WCNC*), Austin, TX, USA, 2022, pp. 405–410.

[15] W. Li, W. Ni, R. Luo, H. Tian, Z. Yang, and C. Huang, Distributed RIS-enhanced cell-free NOMA networks, in *Proc. 2022 IEEE Globecom Workshops* (*GC Wkshps*), Rio de Janeiro, Brazil, 2022, pp. 106–111.

[16] E. Shi, J. Zhang, S. Chen, J. Zheng, Y. Zhang, D. W. K. Ng, and B. Ai, Wireless energy transfer in RIS-aided cell-free massive MIMO systems: Opportunities and challenges, *IEEE Commun. Mag.*, vol. 60, no. 3, pp. 26–32, 2022.

[17] C. Huang, Z. Yang, G. C. Alexandropoulos, K. Xiong, L. Wei, C. Yuen, Z. Zhang, and M. Debbah, Multi-hop RIS-empowered terahertz communications: A DRL-based hybrid beamforming design, *IEEE J. Sel. Areas Commun.*, vol. 39, no. 6, pp. 1663–1677, 2021.

[18] Z. Zhang and Z. Zhao, Weighted sum-rate maximization for multi-hop RIS-aided multi-user communications: A minorization-maximization approach, in *Proc. 2021 IEEE 22$^{nd}$ Int. Workshop on Signal Processing Advances in Wireless Communications* (*SPAWC*), Lucca, Italy, 2021, pp. 106–110.

[19] K. Ardah, S. Gherekhloo, A. L. F. de Almeida, and M. Haardt, Double-RIS versus single-RIS aided systems: Tensor-based MIMO channel estimation and design perspectives, arXiv preprint arXiv: 2109.09099, 2021.

[20] Y. Zhang and C. You, Multi-hop beam routing for hybrid active/passive IRS aided wireless communications, in *Proc. GLOBECOM 2022 – 2022 IEEE Global Communications Conf.*, Rio de Janeiro, Brazil, 2022, pp. 3138–3143.

[21] Z. Zhang, L. Dai, X. Chen, C. Liu, F. Yang, R. Schober, and H. V. Poor, Active RIS vs. passive RIS: Which will prevail in 6G? *IEEE Trans. Commun.*, vol. 71, no. 3, pp. 1707–1725, 2023.

[22] Q. Wu and R. Zhang, Intelligent reflecting surface enhanced wireless network via joint active and passive beamforming, *IEEE Trans. Wireless Commun.*, vol. 18, no. 11, pp. 5394–5409, 2019.

[23] M. Xu, S. Zhang, J. Ma, and O. A. Dobre, Deep learning-based time-varying channel estimation for RIS assisted communication, *IEEE Commun. Lett.*, vol. 26, no. 1, pp. 94–98, 2022.

[24] M. Z. Siddiqi and T. Mir, Reconfigurable intelligent surface-aided wireless communications: An overview, *Intelligent and Converged Networks*, vol. 3, no. 1, pp. 33–63, 2022.

[25] K. Shen and W. Yu, Fractional programming for communication systems—Part I: Power control and beamforming, *IEEE Trans. Signal Process.*, vol. 66, no. 10, pp. 2616–2630, 2018.

[26] S. Boyd, N. Parikh, E. Chu, B. Peleato, and J. Eckstein, Distributed optimization and statistical learning via the alternating direction method of multipliers, https://stanford.edu/~boyd/papers/pdf/admm_distr_stats.pdf, 2014.

[27] D. Shen and L. Dai, Multi-beam design for extremely large-scale RIS aided near-field wireless communications, in *Proc. GLOBECOM 2022 – 2022 IEEE Global Communications Conf.*, Rio de Janeiro, Brazil, 2022, pp. 1–6.

[28] G. Interdonato, E. Björnson, H. Q. Ngo, P. Frenger, and E. G. Larsson, Ubiquitous cell-free massive MIMO communications, *EURASIP J. Wireless Commun. Netw.*, vol. 2019, p. 197, 2019.

**Decai Shen** received the BEng degree (with the highest honor) from Xidian University, Xi'an, China in 2018. He is currently a PhD candidate in electronic engineering at Tsinghua University, Beijing, China. His main research interest is Reconfigurable Intelligent Surface (RIS) with high spectral efficiency transmission. He has received the Honorary Mention in the 2019 IEEE ComSoc Student Competition.



**Zijian Zhang** received the BEng degree in electronic engineering from Tsinghua University, Beijing, China in 2020. He is currently a PhD candidate in electronic engineering at Tsinghua University, Beijing, China. His main research interest is physical-layer algorithms for massive MIMO and RIS. He received the National Scholarship in 2019 and the Excellent Thesis Award of Tsinghua University in 2020.



**Linglong Dai** received the BEng degree from Zhejiang University, Hangzhou, China in 2003, the MEng degree from the China Academy of Telecommunications Technology, Beijing, China in 2006, and the PhD degree from Tsinghua University, China in 2011. From 2011 to 2013, he was a postdoctoral researcher at the Department of Electronic Engineering, Tsinghua University, where he was an assistant professor from 2013 to 2016, an associate professor from 2016 to 2022, and has been a professor since 2022. His current research interests include massive MIMO, RIS, millimeter-wave and Terahertz communications, wireless AI, and electromagnetic information theory. He received the National Natural Science Foundation of China for Outstanding Young Scholars in 2017, the IEEE ComSoc Leonard G. Abraham Prize in 2020, the IEEE ComSoc Stephen O. Rice Prize in 2022, and the IEEE ICC Outstanding Demo Award in 2022. He was elevated as an IEEE fellow in 2021.